Journal of Catalysis **208,** 170–179 (2002)
doi:10.1006/jcat.2002.3561, available online at http://www.idealibrary.com on IDEAL®

Acetic Acid Reduction to Acetaldehyde over Iron Catalysts

II. Characterization by Mössbauer Spectroscopy, DRIFTS, TPD, and TPR

Willy Rachmady and M. Albert Vannice[1]

Department of Chemical Engineering, Pennsylvania State University, University Park, Pennsylvania 16802-4400

Received October 8, 2001; revised February 8, 2002; accepted February 8, 2002

Four catalysts, 1.5% Fe/SiO_2, 3.0% Fe/SiO_2, 5.7% Fe/carbon, and Fe_2O_3, exhibited different phase transformations when subjected to reduction and reaction conditions. After reduction at 673 K in H_2 for 16 h, 31% of the iron in 1.5% Fe/SiO_2 was in superparamagnetic Fe^0 particles with the remainder in Fe^{2+} species, while 3.0% Fe/SiO_2 contained 91% of its iron as α-Fe^0 with the remainder as superparamagnetic Fe^{2+} species. The iron in 5.7% Fe/C existed mostly as α-Fe^0 (63%) with the balance present as Fe^{2+} species, which were mostly superparamagnetic, and the Fe_2O_3 was completely reduced to α-Fe^0. After 8 h on stream, only Fe^{2+} and Fe^{3+} species were detected in 1.5% Fe/SiO_2, which gave only decomposition products; the 5.7% Fe/C catalyst contained α-Fe, Fe^{2+}, Fe^{3+}, and θ-Fe_3C phases and had completely deactivated, and the two active, stable catalysts—3.0% Fe/SiO_2 and Fe_2O_3—showed the presence of both α-Fe and FeO phases under steady-state reaction conditions. It is proposed that the former phase provides sites to activate H_2, and the latter provides different sites to adsorb and activate acetic acid by producing a reactive acetate intermediate. DRIFTS, coupled with TPD and TPR experiments, revealed that surface acetate species are formed during acetic acid adsorption at 300 K on iron surfaces and they appear to be an active intermediate at the reaction temperatures used here. Reaction of this surface acetate with H atoms via a Langmuir–Hinshelwood-type mechanism is proposed to be the principal reaction pathway for acetic acid reduction to acetaldehyde.

INTRODUCTION

Catalytic reduction of aliphatic carboxylic acids with H_2 is of significant interest because it offers a simple and direct route to synthesize industrially important chemicals such as aldehydes, alcohols, and esters. The first part of this study of Fe catalysts (1) and work by others (2–4) reveals that iron can be very selective for the direct reduction of acetic acid with H_2 to form acetaldehyde and water. The kinetics of this reaction over supported iron catalysts can be described using a Langmuir–Hinshelwood-type model invoking one type of site for the activation of hydrogen and another for the adsorption and activation of acetic acid (1). It was proposed that dissociative H_2 adsorption occurs on metallic iron (Fe^0) sites, consistent with previous studies (2, 5, 6), whereas acetic acid adsorption occurs on sites existing on an iron oxide surface to give an active acetate intermediate (1). A similar two-site system has been proposed for this reaction over titania-supported Pt (7, 8).

Although this reaction on Fe and Pt/TiO_2 catalysts can be described using a model involving both metallic and oxidic phases, the differences in the apparent activation energies, activities, and partial pressure dependencies are significant (1). The long induction period required for a reduced Fe catalyst to achieve steady-state activity suggests that the iron undergoes a slow transformation toward an optimum catalytic state during this time. A Mössbauer spectroscopic study of partially reduced Fe_2O_3 by Pestman and coworkers revealed that the catalyst underwent extensive oxidation when subjected to a reaction mixture containing H_2 and acetic acid vapor, and the authors suggested that optimal selectivity to acetaldehyde was obtained when the catalyst surface contained both oxidic and metallic phases of iron (2).

This paper focuses on the characterization of supported iron catalysts utilizing Mössbauer spectroscopy to determine the state of iron after the reduction pretreatment and also after different times on stream. In addition, diffuse reflectance infrared Fourier-transform spectroscopy (DRIFTS) was combined with temperature-programmed desorption (TPD) and temperature-programmed reaction (TPR) to identify surface species and examine their stability and reactivity. These techniques were employed to obtain a better understanding of the catalytic chemistry associated with this reaction over iron catalysts.

EXPERIMENTAL

Silica-supported and carbon-supported Fe catalysts were prepared using an incipient wetness technique and were characterized using CO and H_2 chemisorption and XRD, as previously described (1). These catalysts were subjected

[1] To whom correspondence should be addressed. E-mail: mavche@engr.psu.edu.

0021-9517/02 $35.00

to a standard reduction pretreatment which involved heating at 3 K/min to 673 K under 1 atm of flowing H_2 (50 cm^3(STP)/min) and holding at this temperature for 16 h. Based on CO adsorption assuming a stoichiometry of $CO_{ad}/Fe_s = 1/2$, where Fe_s is a surface Fe atom, iron dispersions of 0.64, 0.07, and 0.15 were measured for 1.5% Fe/SiO_2, 3.0% Fe/SiO_2, and 5.7% Fe/carbon, respectively, while the metallic iron site density on Fe_2O_3 (Alfa Aesar, 99.998%) obtained following the reduction treatment was 8.4 μmol of Fe_s/g, which gives a dispersion of 0.0007 if all the iron is assumed to be reduced (1).

The catalysts were subjected to standard reaction conditions in which acetic acid (HOAc) reduction was carried out with H_2 at a selected temperature, typically 553 K, in the vapor phase at atmospheric pressure. The partial pressures of HOAc and H_2 in the feed were 14.7 and 700 Torr, respectively, with He as the balance gas.

Constant-acceleration Mössbauer spectra were obtained at room temperature using an Austin Science Associates, Inc., S-600 Mössbauer controller and a personal computer equipped with a PCA-II multichannel analyzer. The source was comprised of 30 mCi of ^{57}Co diffused into a Rh matrix. The spectra were calibrated using a 12.5-μm NBS Fe foil, and the fitted spectral parameters are reported with respect to this standard absorber. The absorption data were fit using a modification of the MFIT program (9), with sextuplet intensities constrained to the expected ratios and doublets constrained for symmetry and equal dip/width (10). A reactor/absorber cell equipped with low Fe-content Be windows for high γ-ray transmission was constructed using 316L stainless steel. In addition to the collection of Mössbauer spectra, the cell allowed *in situ* pretreatments and reactions to be carried out at temperatures as high as 723 K.

DRIFT spectra were obtained using an FTIR spectrometer (Mattson Instrument, RS-1000) equipped with a diffuse reflectance IR spectroscopy cell (Harrick Scientific, HVC-DR2) and a praying mantis mirror assembly (Harrick Scientific, DRA-2-CO), which was modified to allow *in situ* catalyst pretreatments or reactions with accurate temperature measurement (11). Infrared spectra of adsorbed species were collected at atmospheric pressure and temperatures from 298 to 473 K at a resolution of 4 cm^{-1}. Unless noted otherwise, all spectra were referenced to the freshly reduced catalyst sample at the identical temperature in flowing Ar prior to introduction of the adsorbate.

TPD and TPR experiments were conducted using a glass microreactor connected to a quadrupole mass spectrometer (UTI Instruments) for generating the desorption curves. Up to 15 mass numbers could be simultaneously monitored during each run and their respective signal intensities were recorded and reported without correction for sensitivity factors. The heating rate was 20 K/min with 50 cm^3(STP)/min He or H_2 as the carrier gas. The effects of concentration gradients and lag times in the sample cell and in the catalyst pores were evaluated using criteria discussed by Gorte (12).

Acetic acid (E.M. Science, 99.7% glacial) and acetaldehyde (Aldrich, 99.5+%) were degassed by freeze–thaw cycles in an inert atmosphere before use, and vapor-phase HOAc or acetaldehyde was introduced to the adsorption/reactor cell by bubbling the carrier gas through either liquid held in a saturator at 273 K. H_2 (MG Ind., 99.999%), He (MG Ind., 99.999%), and Ar (MG Ind., 99.999%) were further purified using separate in-line molecular sieve traps (Supelco) and Oxytraps (Alltech Asso.) for each gas.

RESULTS

Figures 1 through 4 represent Mössbauer spectra of 3.0% Fe/SiO_2, 5.7% Fe/Carbon, 1.5% Fe/SiO_2, and Fe_2O_3 after being subjected to the standard reduction pretreatment and standard reaction conditions at 553 K. All spectra were collected at room temperature following each treatment with the sample under flowing He, and the solid lines drawn through the data points are the optimized fits obtained with the corresponding spectral parameters listed in Table 1.

A 16-h reduction at 673 K converted only 91% of the iron precursor in 3.0% Fe/SiO_2 into α-Fe, which is characterized by the six-line pattern in Fig. 1, spectrum a, with a hyperfine field (HF) of 331 kOe. The remaining 9% was in the form of superparamagnetic Fe^{2+}, as evidenced by a

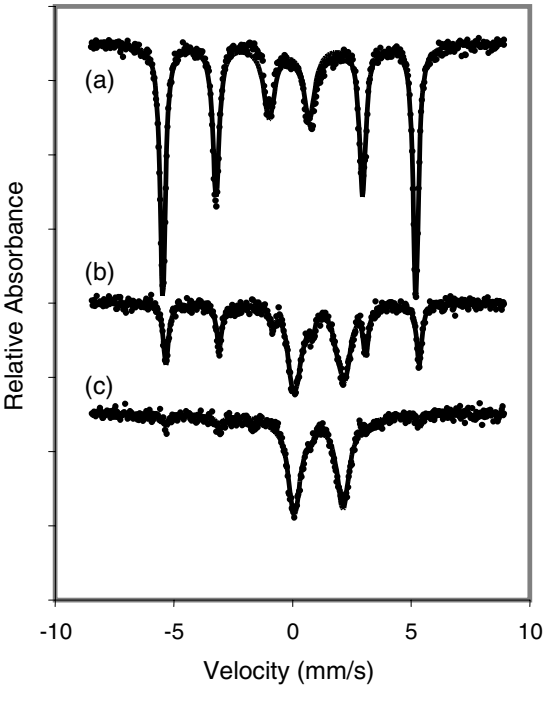

FIG. 1. Mössbauer spectra of 3.0% Fe/SiO_2 at room temperature: (a) after reduction at 673 K; (b, c) after 8 min and 8 h of reaction at 553 K, respectively.

TABLE 1

Mössbauer Spectral Parameters for Iron Catalysts[a]

Catalyst	Treatment	Phase	IS (mm/s)	QS (mm/s)	HF (kOe)	SC (%)
3% Fe/SiO_2[b]	After reduction at 673 K for 16 h	α-Fe	0.0	0.0	331	91
		s.p. Fe^{2+}	0.90	—	—	9
	After 8 min of reaction at 553 K	α-Fe	0.0	0.0	331	46
		Fe^{2+}	1.18	2.07	—	64
	After 8 h on stream at 553 K	α-Fe	0.0	0.0	332	13
		Fe^{2+}	1.11	2.05	—	83
		Fe^{3+}	0.34	0.72	—	4
5.7% Fe/C[c]	After reduction at 673 K for 16 h	α-Fe	0.0	0.0	331	63
		s.p. Fe^{2+}	0.93	—	—	33
		Fe^{2+}	1.03	2.21	—	4
	After 8 min of reaction at 553 K	α-Fe	0.0	0.0	330	64
		s.p. Fe^{2+}	0.97	—	—	26
		Fe^{2+}	0.99	1.96	—	4
		Fe^{3+}	0.29	0.58	—	5
	After 8 h on stream at 553 K	α-Fe	0.0	0.0	331	54
		s.p. Fe^{2+}	1.01	—	—	1
		Fe^{2+}	1.06	1.99	—	7
		Fe^{3+}	0.16	0.87	—	7
		θ-Fe_3C	0.20	0.02	208	31
1.5% Fe/SiO_2[d]	After reduction at 673 K for 16 h	s.p. Fe^0	0	—	—	31
		Fe^{2+}	0.99	2.02	—	39
		Fe^{2+}	0.97	0.34	—	30
	After 1 h onstream at 553 K	Fe^{2+}	1.14	1.99	—	24
		Fe^{3+}	0.36	0.99	—	76
Fe_2O_3[e]	After reduction at 673 K for 16 h	α-Fe	0.0	0.0	330	100
	After 8 min of reaction at 553 K	α-Fe	0.0	0.0	330	100
	After 8 h onstream at 553 K	α-Fe	0.0	0.0	329	96
		Fe^{2+}	0.98	2.13	—	3

[a] IS, Isomer shift; QS, quadrupole splitting; HF, hyperfine field; and SC, spectral contribution.
[b] As shown in Fig. 1.
[c] As shown in Fig. 2.
[d] As shown in Fig. 3; s.p. = superparamagnetic.
[e] As shown in Fig. 4.

singlet at 0.9 mm/s. After 8 min under reaction conditions, a significant amount of α-Fe was transformed into Fe^{2+}, as exhibited by the appearance of a doublet in spectrum b (Fig. 1) which had an a isomer shift (IS) of 1.18 mm/s and a quadrupole splitting (QS) of 2.07 mm/s. A doublet with similar IS and QS values has been associated with Fe^{2+} iron in a high-coordination environment, such as in bulk iron (9, 13). Spectrum c (Fig. 1) was collected after 8 h on stream; thus it contains information regarding the catalyst phase compositions at steady-state conditions. The amount of metallic iron had decreased to 13%, with the remainder existing in oxidic forms, i.e., in addition to the Fe^{2+} species, the spectrum contained another doublet, with an IS of 0.34 mm/s and a QS of 0.72 mm/s, characteristic of Fe^{3+} species, which accounted for 4% of the spectral area.

A similar series of experiments with 5.7% Fe/carbon produced the Mössbauer spectra displayed in Fig. 2 and gave the parameters listed in Table 1. After the standard reduction pretreatment, 63% of the iron was present as α-Fe, as estimated from the spectral contribution of the sextuplet, with the remaining iron existing as both superparamagnetic Fe^{2+} species, which are depicted by a singlet at 0.97 mm/s, and another Fe^{2+} species depicted by a doublet with an IS of 1.03 mm/s and a QS of 2.21. Similar parameters have been reported previously for carbon-supported iron catalysts (14). The spectrum changed slightly after the catalyst was subjected to standard reaction conditions for 8 min, and an additional doublet, with an IS of 0.29 mm/s and a QS of 0.58 mm/s, developed and accounted for about 5% of the total spectral area. This doublet can be attributed to Fe^{3+} species. Major changes occurred in the catalyst after 8 h onstream, as indicated by spectrum c (Fig. 2), and a form of iron carbide undoubtedly developed in the catalyst because the spectrum shows the presence of an additional set of sextuplets having smaller widths than that of α-Fe. The spectrum was fitted with different combinations of the α-Fe

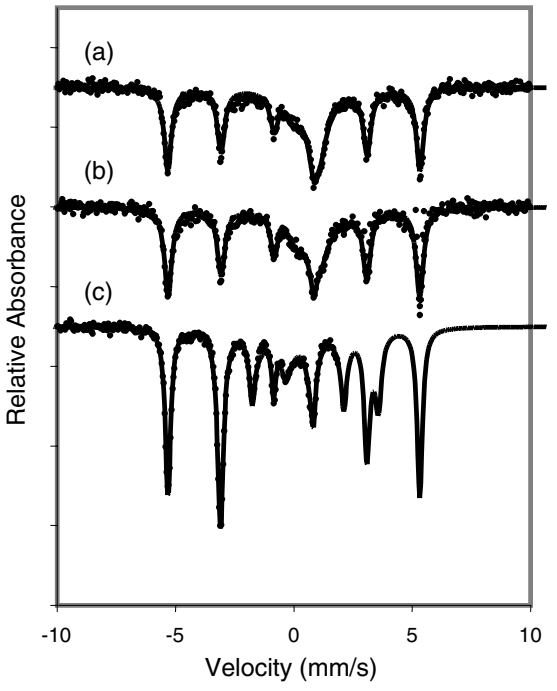

FIG. 2. Mössbauer spectra of 5.7% Fe/C at room temperature: (a) after reduction at 673 K; (b, c) after 8 min and 8 h of reaction at 553 K, respectively.

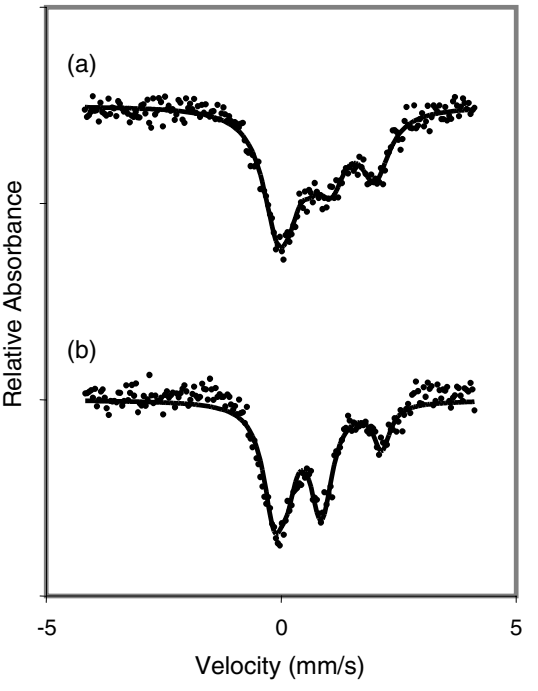

FIG. 3. Mössbauer spectra of 1.5% Fe/SiO_2 at room temperature: (a) after reduction at 673 K and (b) after 1 h of reaction at 280 K.

sextuplet and those associated with four types of carbides, i.e., ε'-$Fe_{2.2}C$, ε-F_2C, χ-Fe_5C_2, and θ-Fe_3C, and physically meaningful parameters were obtained only when sextuplets of Fe^0 and θ-Fe_3C were simultaneously fitted, which gave the spectral parameters listed in Table 1. The IS value obtained for θ-Fe_3C is lower than that reported by Bernas and Campbell (15), but it is very similar to the value reported by Badani and Delgass (16).

The 1.5% Fe/SiO_2, which was found to be inactive for acetic acid reduction (1), was subjected to the standard reduction pretreatment and subsequently to standard reaction conditions for 1 h. The Mössbauer spectrum of the catalyst following the pretreatment step, shown in Fig. 3, spectrum a, does not indicate the presence of α-Fe, as evidenced by the absence of the corresponding sextuplet. Instead, highly dispersed iron was detected because the spectrum can be fit using the superparamagnetic Fe^0 phase, which has a singlet with an IS value of 0.0 mm/s, plus high- and low-coordination Fe^{2+} species, which have doublets with the spectral parameters listed in Table 1. The Mössbauer spectrum of the catalyst after 1 h on stream, shown in spectrum b (Fig. 3), consists mainly of an Fe^{2+} doublet, with an IS of 1.14 mm/s and a QS of 1.99 mm/s, and an Fe^{3+} doublet with an IS of 0.36 mm/s and a QS of 0.99 mm/s.

The behavior of unsupported iron was investigated by following the changes in the Mössbauer spectrum of Fe_2O_3, which was also reduced at 673 K for 16 h and subsequently subjected to reaction conditions at 553 K for 8 min and then for another 8 h. Spectrum a in Fig. 4 shows that Fe_2O_3 was completely converted to metallic Fe after the reduction pretreatment, as evidenced by the characteristic six-line pattern, and after 8 min under reaction conditions there was no discernable change, as shown by spectrum b (Fig. 4).

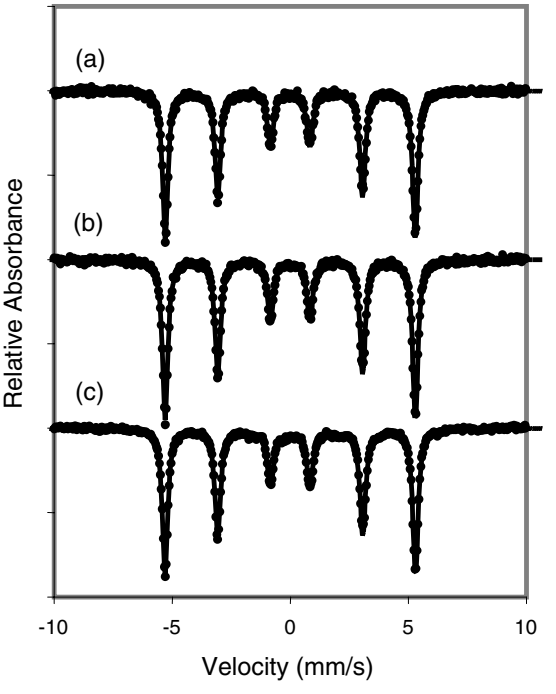

FIG. 4. Mössbauer spectra of Fe_2O_3 at room temperature: (a) after reduction at 673 K; (b, c) after 8 min and 8 h of reaction at 553 K, respectively.

After 8 h on stream, a doublet with an IS of 0.98 mm/s and a QS of 2.13 mm/s (characteristic of an Fe^{2+} species) finally emerged which accounted for about 3.0% of the total spectral area.

Infrared spectra of surface species were collected after flowing acetic acid or acetaldehyde vapor through the DRIFTS cell for 30 min and then purging the cell with flowing Ar or He for 90 min. The cell was maintained at atmospheric pressure and 300 K during both the adsorption process and the purging step. Figure 5 shows DRIFT spectra for both 3.0% Fe/SiO_2 and the pure silica support. Three different species can be identified on the catalyst surface, i.e., adsorbed molecular HOAc, a silyl ester, and an acetate species. The HOAc is characterized by IR bands at 1728 cm^{-1} for ν(C=O) and 930 cm^{-1} for γ(O–H), which are observed following adsorption on either 3.0% Fe/SiO_2 or the pure silica support, and the broad band at 3366 cm^{-1} is indicative of HOAc adsorbed on the silica surface via hydrogen bonding. The interaction between the lone electron pair on the carbonyl oxygen atom in HOAc and the hydrogen in the hydroxyl group on the SiO_2 surface causes a large shift in the ν(O–H) band to lower frequencies and a loss of intensity in the IR band at 3743 cm^{-1} for free hydroxyl groups on silica, as exhibited in the spectra. Finally, a large red shift in the ν(C=O) wavenumber for adsorbed HOAc, relative to the same frequency in vapor-phase HOAc, also indicates that it is bonded to the hydroxyl group through its carbonyl oxygen.

The shoulder at 1748 cm^{-1} is characteristic of ν(C=O) in silyl ester species formed by dissociative HOAc adsorption on SiO_2 surfaces and is in accordance with the observations by Jackson *et al.* (17). Infrared bands at 1572 and 1426 cm^{-1} are attributed to species adsorbed on iron because they do not appear in the spectrum of HOAc adsorbed on pure silica, and from their positions and splitting, they can be assigned to a surface acetate species on iron which has a band at 1426 cm^{-1} for ν_s(COO) and one at 1572 cm^{-1} for ν_a(COO) (18). The distance between the asymmetric and symmetric stretching frequencies is close to the ionic values; thus it suggests that this acetate species is bound to the surface, with each oxygen atom interacting with a different metal atom, i.e., in a bridging configuration (19).

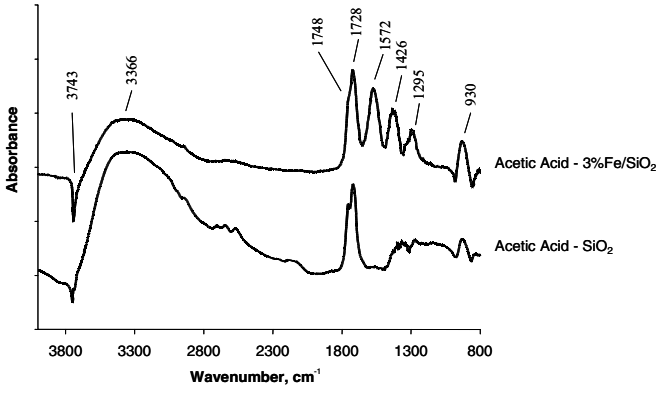

FIG. 5. DRIFT spectra following acetic acid adsorption on 3.0% Fe/SiO_2 or SiO_2 at 300 K and purging in Ar.

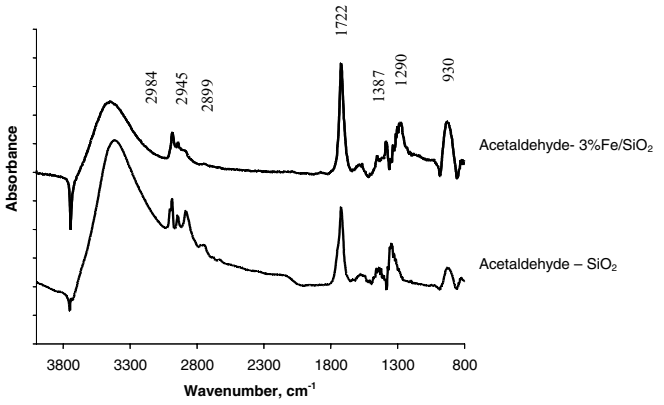

FIG. 6. Drift spectra of adsorbed species after acetaldehyde adsorption on 3.0% Fe/SiO_2 and SiO_2 at room temperature.

Spectra of the 3.0% Fe/SiO_2 catalyst following acetaldehyde adsorption were also obtained because acetaldehyde is the main product of acetic acid reduction over Fe (1–4). In general, the spectra obtained after acetaldehyde adsorption on either 3.0% Fe/SiO_2 or pure SiO_2 were similar, as shown in Fig. 6, and they consisted of IR bands characteristic of molecular adsorption on a silica surface. Acetaldehyde also adsorbs via hydrogen bonding between its carbonyl oxygen and a surface hydroxyl group, as evidenced by the IR absorption profile between 3000 and 3800 cm^{-1} and the large red shift in the ν(C=O) stretch frequency. The assignments for the principal bands are as follows: 2984, 2945, and 2899 cm^{-1} for ν(C–H), 1722 cm^{-1} for ν(C=O), 1387 cm^{-1} for δ(C–H), 1290 cm^{-1} for ν(C–O), and 930 cm^{-1} for γ(OH) (20). The spectra also show weak bands at 1583 and 1454 cm^{-1} which are similar to the IR absorption bands associated with the carboxylate group stretching frequencies of surface acetate species.

Figure 7 displays spectra which were recorded intermittantly between 1 and 120 min on stream during acetic acid hydrogenation over 3.0% Fe/SiO_2 at 553 K. Gradual changes are apparent in the two regions between 1400–2200 and 2700–3200 cm^1. As time on stream increases, the latter region showed increasing intensity at 2984, 2945, and 2899 cm^{-1}, which represent bands attributed to ν(C–H) frequencies characteristic of molecular acetaldehyde adsorbed on a silica surface via hydrogen bonding. Thus the acetaldehyde coverage on the silica surface increased slowly during the first few hours of reaction along with the rate of acetaldehyde formation during this period of time, which is consistent with the kinetic behavior reported previously (1). The spectral changes in the 1400- to 2200- cm^{-1} region are more complex because changes in the baseline occurred due to oxidation of iron; nonetheless, these spectral changes are

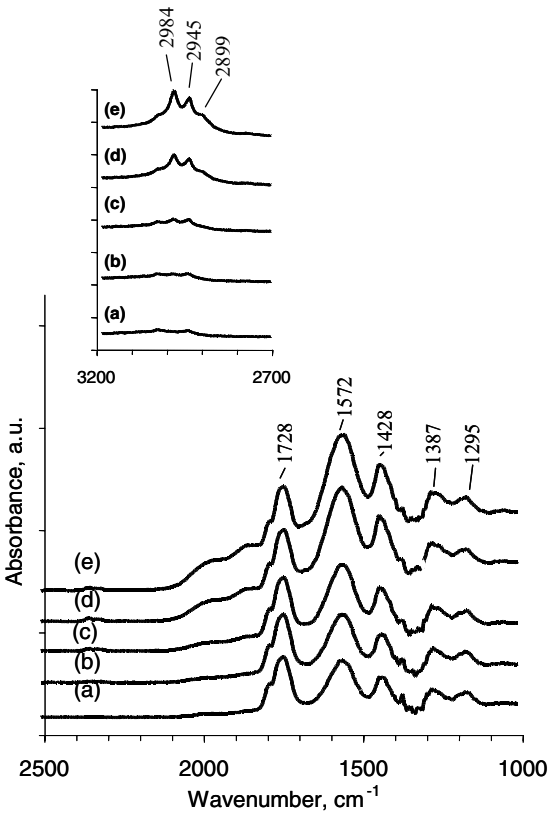

FIG. 7. DRIFT spectra during acetic acid hydrogenation over 3.0% Fe/SiO_2 at 553 K after (a) 1, (b) 6, (c) 20, (d) 72, and (e) 120 min on stream.

consistent with the Mössbauer spectroscopic results showing that iron underwent partial oxidation during the early period on stream.

Information regarding the thermal stability of surface species and their decomposition patterns was obtained from TPD experiments. Prior to a TPD run, the catalyst surface was saturated with acetic acid by flowing the vapor through the cell and then purging the sample at room temperature. Figure 8 shows the TPD spectra after HOAc adsorption on 3.0% Fe/SiO_2. The DRIFT spectra of this catalyst after stepwise heating to 373, 473, 573, 673, or 773 K in flowing Ar followed by cooling to 300 K are shown in Fig. 9. The resulting TPD spectra show peaks at 420 and 673 K, with the first peak due to the desorption of molecular HOAc. This desorption is in accordance with the disappearance of the IR band at 1724 cm^{-1} after heating the catalyst to 473 K, as shown in Fig. 9, because this band was assigned to the C=O stretching frequency of hydrogen-bonded HOAc. The peaks for methane ($m/e = 15, 16$), CO_2 ($m/e = 44$), acetaldehyde ($m/e = 29$), ethylene ($m/e = 27$), ketene ($m/e = 14, 42$), and acetone ($m/e = 43$) that evolve at 673 K represent products coming from decomposition reactions on the surface. No molecular HOAc desorption at 673 K was detected, and desorption of H_2, H_2O, and CO is not reported because the signals at $m/e = 2$, 18, and 28 could not be resolved from the background. The similar peak temperature for these six products suggests that they were derived from the same surface species, and these products are similar to those obtained during the decomposition of acetate species on a reduced

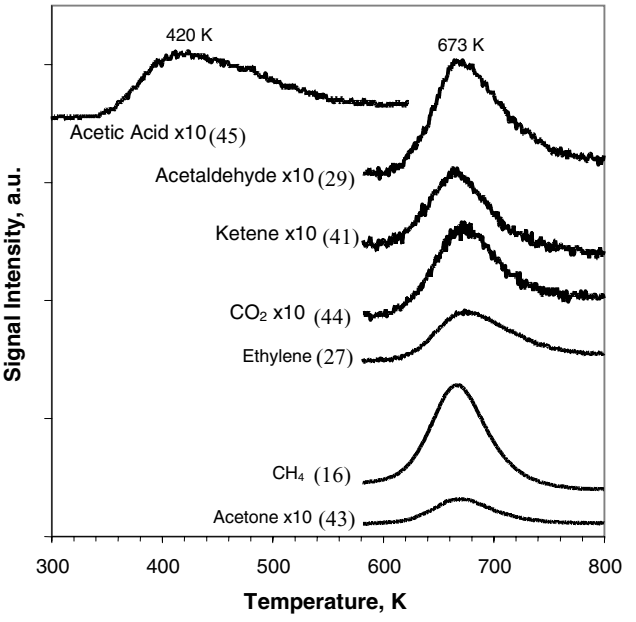

FIG. 8. TPD spectra after acetic acid adsorption on 3.0% Fe/SiO_2 at 300 K.

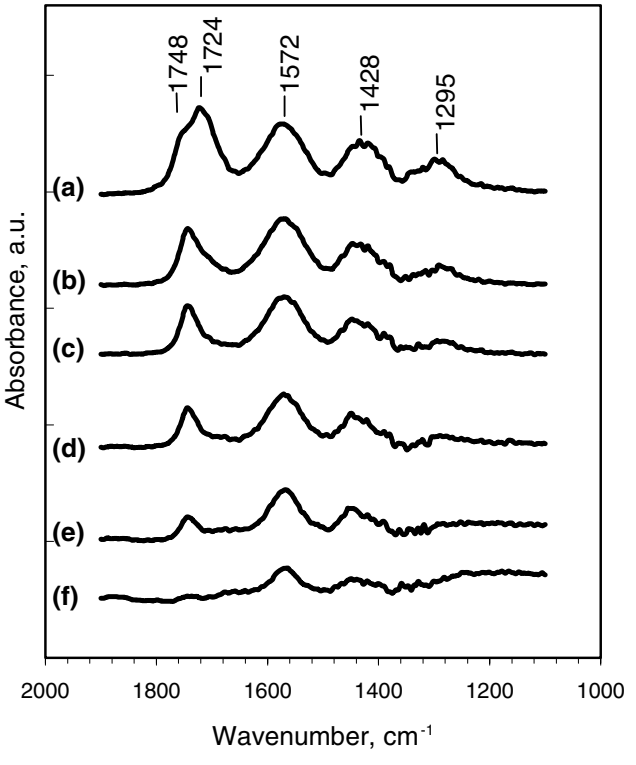

FIG. 9. Decomposition of acetate and silyl esters on 3.0% Fe/SiO_2. Spectra recorded at 300 K after stepwise heating in flowing Ar to (a) 300, (b) 373, (c) 473, (d) 573, (e) 673, and (f) 773 K.

titania surface (21). In addition, a separate TPD experiment with pure silica showed that silyl ester decomposition occurred at a slightly higher temperature of 700 K; therefore, the TPD peaks at 673 K are attributed to the decomposition of surface acetate species on iron. The reactivity of these surface species can be evaluated by the TPR run because H_2 was used as the carrier gas. As in the TPD experiment, the catalyst surface was saturated with acetic acid and then purged at room temperature prior to the TPR run. Figure 10 shows the results for species adsorbed on 3.0% Fe/SiO_2, and these spectra exhibit desorption peaks for HOAc at 420 and 550 K, CO_2 at 550 K, acetaldehyde and ethanol at 560 K, ethylene at 580 K, and CH_4 at 590 K. Acetone and ketene were not detected. In addition to having HOAc desorb at 550 K and ethanol desorb at 560 K, desorption peaks for acetaldehyde, ethylene, CH_4, and CO_2 were at much lower temperatures than those obtained in the TPD experiments, but these differences in products and peak temperatures are consistent with the expected reactions between adsorbed hydrogen and the surface species present.

Figure 11 shows the corresponding IR spectra for 3.0% Fe/SiO_2 following stepwise heating in flowing hydrogen. The disappearance of almost all of the IR bands after heating to 673 K is consistent with the TPR results, which showed that reactions between the surface organic species and hydrogen indeed occur below this temperature. Acetaldehyde and ethanol represent products of the reaction between hydrogen and surface acetate species given the fact that they were not observed in the TPR run conducted with the silica support alone. The acetic acid peak at 550 K arises from the recombination of hydrogen with surface acetate and/or silyl ester species.

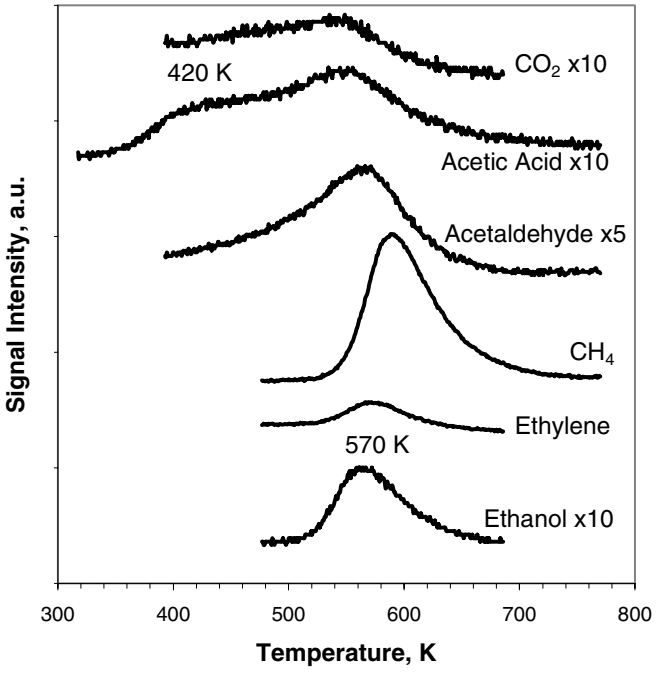

FIG. 10. TPR spectra after adsorption of acetic acid on 3.0% Fe/SiO_2 at 300 K.

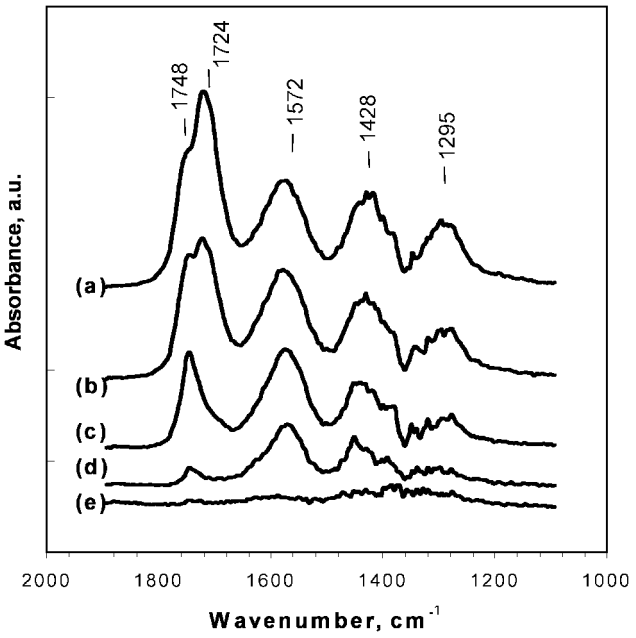

FIG. 11. Decomposition and reduction of acetate and silyl esters on 3.0% Fe/SiO_2. Spectra recorded at 300 K after stepwise heating in flowing H_2 to (a) 300, (b) 373, (c) 473, (d) 573, and (e) 673 K then cooling.

DISCUSSION

The four iron catalysts investigated in the present study, i.e., highly and moderately dispersed iron on silica (1.5% Fe/SiO_2 and 3.0% Fe/SiO_2, respectively), carbon-supported iron, and unsupported Fe_2O_3 powder, exhibited markedly different phase transformations when subjected to reduction and reaction conditions. As indicated by the Mössbauer spectra obtained after the reduction pretreatment, the ease of reducibility can be ordered as follows: $Fe_2O_3 > 3.0\%$ $Fe/SiO_2 > 5.7\%$ Fe/carbon $> 1.5\%$ Fe/SiO_2. In the last catalyst, prepared by impregnation with a solution of $Fe_3(CO)_{12}$ in THF containing the metal in the zero-valent state, the iron appeared to be partially oxidized during drying and wafer preparation, as indicated by its orange color. Complete reduction to metallic iron is difficult with very small iron particles on silica (22), and the reduction pretreatment used here did not convert all the highly dispersed iron on 1.5% Fe/SiO_2 into a zero-valent form. However, any water remaining on the support as well as that generated by dehydroxylation of the silica surface during the reduction pretreatment could also be responsible for the oxidized state of iron (23). Kock and Geus have also suggested that small iron particles tend to have a more open surface due to a displacive surface rearrangement (22); as a result, oxygen atoms cannot be as easily removed by a reduction

treatment, an explanation that was corroborated by the work of Vink *et al.* (24, 25). In addition, the type of support can play a major role in dictating the ease of iron reduction, as shown by comparative studies with silica-, alumina-, and magnesia-supported iron (25–28) and a study with carbon-supported iron (13). In general, the stronger the interaction between iron and the support surface, the more difficult the reduction of the metal. Since this support effect can be significant with small Fe particles, complete reduction at low temperatures may not occur. Regardless of whether or not such a support effect is dominant, iron reducibility is also found to be greatly dependent on particle size, and from a phenomenological standpoint, larger particle sizes of oxidized Fe are easier to reduce than very small ones. The order of reducibility mentioned earlier for the four catalysts examined here follows this trend.

Catalytic behavior is also distinctly different among these catalysts. Fe_2O_3 and 3.0% Fe/SiO_2 showed a relatively long induction period after which stable activity was maintained. On the other hand, 5.7% Fe/carbon deactivated very rapidly and never stabilized while 1.5% Fe/SiO_2 failed to show any measurable activity (1). The Mössbauer spectra obtained after these catalysts were subjected to reaction conditions revealed significant phase transformations within the iron particles. Under steady-state reaction conditions, Fe_2O_3 and 3.0% Fe/SiO_2 were composed of both metallic and oxidic phases of iron, whereas 5.7% Fe/carbon underwent significant carburization with time on stream and 1.5% Fe/SiO_2 was further oxidized so that only Fe^{2+} and Fe^{3+} phases were detected. Iron catalysts that work well in this reaction seem to possess both α-Fe and ferrous oxide phases under reaction conditions, which agrees with the view that acetic acid hydrogenation requires both metallic sites to activate hydrogen and oxidic sites to form an active form of HOAc (1–3, 7, 8). During the induction period, some of the metallic iron was oxidized by HOAc. Upon interaction with H_2 at an appropriate set of conditions, a portion of the surface can be re-reduced to metallic iron; however, this may not always be uniform throughout the catalyst surface because the reduction process has been frequently shown to be structure sensitive. As indicated by studies of Fe single-crystal surfaces (24, 25), reduction of a more open surface structure, such as Fe (100), is more difficult than that of the close-packed Fe (110) surface. This is just one example of how the degree of reduction or re-reduction can be affected by surface structure, which can vary significantly with small particles. Fortunately, for the HOAc reduction sequence, the oxidic iron phase provides one type of active site required in this reaction but, at the same time, metallic iron sites also need to be maintained at the surface. Based on this analysis, it can be seen qualitatively how the particle size may affect metallic and oxidic site concentrations. Unfortunately, the Mössbauer results cannot provide information specifically about the surface phase compositions of the active catalysts because the large iron particles in the catalysts had very low surface/volume ratios; thus, an explanation of the apparent particle size effect on iron surface composition remains speculative until definitive evidence is obtained. Nonetheless, if the surface composition of the iron surface mirrors that of the bulk, then the surface is transformed into mixed phases of iron as time on stream increases (note that the spectral fraction of Fe^{+2} is 0.03 while the fraction of surface Fe atoms is only 0.0007). Thus at steady-state reaction conditions, the reaction can proceed via a Langmuir–Hinshelwood-type mechanism involving both metallic and oxidic sites. As more neighboring Fe^0 and Fe^{2+} species are established, the rate of HOAc reduction increases, as implied by the activity profiles for Fe_2O_3 and 3.0% Fe/SiO_2 provided in the preceding paper (see Fig. 1) (1).

Carburization appears to be responsible for the deactivation observed with the 5.7% Fe/carbon catalyst. The formation of bulk carbide has been recognized to be responsible for iron catalyst deactivation in the Fischer–Tropsch synthesis (29) and this deactivation is a good indication of the presence of carbon atoms on the surface (30). The amount of surface carbon can become excessive after long periods of time on stream, during which more metallic iron is converted into carbides and carbon diffusion into the bulk becomes slower. This surface carbon is detrimental to catalyst activity, as it permanently blocks reaction sites, particularly those required to activate hydrogen, as in the case of HOAc reduction. The 5.7% Fe/carbon is the only catalyst that simultaneously exhibited deactivation (1) and carbide formation and it seems logical that the former results from the latter. There is no indication that a similar process occurred in the silica-supported catalyst or in the unsupported Fe_2O_3, which suggests carburization may be facilitated by the use of a carbon support; however, it is not believed that the carbon originated from the support because the reaction temperature was too low to facilitate such carbon transport. This leaves either acetic acid, one of its hydrogenated products, or one of its decomposition products as the principal source of carbon atoms. Although the source of the carbon is not known at this time, these results suggest that a carbon support can influence the behavior of iron, perhaps because of a weak interaction between Fe and the carbon surface in small micropores.

The 1.5% Fe/SiO_2 catalyst, which consisted of highly dispersed iron, was very susceptible to oxidation because after a 1-h exposure to the reaction mixture, there was no metallic iron detected. Under these reaction conditions, oxidation of these small Fe particles was extensive and may have been irreversible because the surface structure would be more open and, consequently, more difficult to re-reduce, thus resulting in no detectable hydrogenation activity with this catalyst. The absence of reduction activity observed by Cressely *et al.* with their Fe/SiO_2 sample may have been due to similar behavior (31).

Although the surface composition can be associated with catalyst activity, it is difficult to obtain quantitative information about the surface structure of these catalysts. Except for 1.5% Fe/SiO_2, Mössbauer spectral contributions from the surface atoms cannot be distinguished because they constitute a small fraction of the atoms in large iron particles; therefore, more-elaborate surface-sensitive techniques are required. Despite the absence of this important information, Mössbauer spectroscopy has shown that iron undergoes significant phase transformations during reaction, and the extent and nature of this phase transformation determines the catalytic behavior. Furthermore, the activity versus time on stream profile is consistent with the proposed catalytic system, which involves both metallic and oxidic phases of iron.

The identification of surface species and their role in this reaction is an integral part of gaining insight into the mechanistic details of HOAc reduction. DRIFT spectra obtained after HOAc adsorption at 300 K and under reaction conditions reveal that bidentate acetate species are formed on iron surfaces, while molecularly adsorbed HOAc and silyl esters are found only on the silica surface. There are no apparent differences between the IR absorption bands for the acetate species on metallic iron and those on oxidized iron because similar IR bands are obtained at 300 K and during reaction at 553 K. TPD of surface species on silica reveals that molecular HOAc desorbs intact, with a peak at 420 K, while the silyl ester decomposes at 700 K. Products detected during TPR of adsorbed HOAc and the silyl ester in H_2 do not include either acetaldehyde or ethanol, which implies that neither molecularly adsorbed HOAc nor a silyl ester is involved in the hydrogenation sequence. The acetate species, on the other hand, appear to be active surface intermediates, and acetaldehyde is detected as one of the TPD products of acetate decomposition, with a peak at 673 K. Under TPR conditions, the acetate species react with hydrogen to produce acetaldehyde and ethanol, with this reactivity beginning around 500 K and reaching a maximum at 570 K. The temperatures at which acetate hydrogenation activity is observed in the TPR experiment are similar to those used in the steady-state reaction studies (1).

Acyl species, which were invoked as active intermediates in this reaction on Pt/TiO_2 catalysts (21), were not detected on the iron surface. Considering that acyl species are more reactive than acetate species and their surface coverage at reaction temperatures is probably very low, if they are present at all, any acetaldehyde formation via acyl hydrogenation appears to be minimal under the reaction conditions required here; therefore, it is proposed that HOAc reduction over iron takes place predominantly via hydrogenation of an acetate species via a Langmuir–Hishelwood-type mechanism in which hydrogen atoms adsorbed on metallic sites combine with a bridging acetate species adsorbed on an oxidic site to produce adsorbed acetaldehyde and water. Pei and Ponec have previously proposed that an acetate species is an active intermediate in this reaction on Pt/SnO_2 and Pt/TiO_2 catalysts (32). DRIFT spectra after acetaldehyde adsorption on Fe/SiO_2 reveal that the surface coverage of acetaldehyde on iron is not significant. In addition, the rather high temperatures at which the reaction takes place favor desorption of acetaldehyde relative to further hydrogenation to ethanol; consequently, subsequent hydrogenation of acetaldehyde to ethanol is not as extensive as on Pt/TiO_2, thereby maintaining a high selectivity to acetaldehyde.

Ponec and coworkers have suggested another possible pathway by which acetic acid may be catalytically reduced over solid surfaces, and it invokes a Mars-Van Krevelen-type mechanism in which acetic acid adsorbs at oxygen vacancies, such as those created on reducible oxide surfaces, and loses one oxygen atom directly to the lattice to form acetaldehyde (2, 8, 33). The catalytic cycle is completed when hydrogen removes this oxygen atom via water formation. This proposal was based on a conclusion by these authors that oxygen vacancies were necessary for the selective reduction of HOAC to acetaldehyde. Acetic acid hydrogenation via a Mars–Van Krevelen mechanism would involve the loss of an O atom to fill a lattice vacancy; thus, it should be a process similar to that which formed acetaldehyde during the TPD experiments. However, the temperature (ca. 673 K) at which this occurred during these experiments was much higher than that for our steady-state reaction conditions; thus, it seems unlikely that acetaldehyde (and ethanol) formation at lower temperature proceeds by this type of mechanism. In fact, in the TPR experiments in which surface reactions were simulated, acetaldehyde and ethanol were evolved at a temperature similar to that used at steady-state reaction conditions. Furthermore, the fact that freshly reduced Fe catalysts show an initial activity that is lower than the steady-state activity does not support the Mars–Van Krevelen mechanism because there should be more oxygen vacancies on the catalyst surface after the reduction pretreatment than after several hours on stream. Hence, in view of the above considerations and the kinetic modeling discussed previously (1), the Langmuir–Hinshelwood mechanism is preferred for describing HOAc reduction over Fe catalysts.

The reaction temperature required for these Fe/SiO_2 catalysts is much higher compared to that needed for our Pt/TiO_2 catalysts. The partial pressure study with 3.0% Fe/SiO_2 showed that the rate dependence on H_2 pressure is between first and second order, while the rate is almost independent of the HOAc partial pressure. These results contrast markedly with the respective reaction orders observed for Pt/TiO_2 (7). Finally, the apparent activation energy with Fe/SiO_2 is twice that with Pt/TiO_2. More thermally stable intermediates, such as surface acetate species, would require higher temperatures compared to a more

reactive intermediate, such as an acyl species; thus, invoking an acetate species as a principal reaction intermediate for this reaction over iron catalysts is consistent with the higher temperature requirement. A kinetic model invoking addition of the second hydrogen atom to the acetate complex as the slow step is also consistent with experimental observations (1). Consequently, the observed differences in catalytic behavior between Pt/TiO_2 and Fe/SiO_2 can be explained by invoking a different reaction intermediate and by shifting the rate-determining step in regard to the addition of H atoms to this intermediate (1).

SUMMARY

The four catalysts, 1.5% Fe/SiO_2, 3.0% Fe/SiO_2, 5.7% Fe/carbon, and Fe_2O_3, exhibited different phase transformations when subjected to reduction and reaction conditions. The active catalysts showed the presence of both α-Fe and FeO phases during reaction under steady-state conditions, and it is proposed that the former provides sites to activate H_2 and the latter provides different sites to adsorb and activate HOAc by producing a reactive acetate intermediate. DRIFTS, coupled with TPD and TPR experiments, revealed that surface acetate species are formed during acetic acid adsorption at 300 K on iron surfaces and they appear to be an active intermediate. Reaction of this surface acetate with H atoms via a Langmuir–Hinshelwood-type mechanism is proposed to be the principal reaction pathway for HOAc reduction by H_2 to acetaldehyde.

REFERENCES

1. Rachmady, W., and Vannice, M. A., *J. Catal.* **208**, 158 (2002).
2. Pestman, R., Koster, R. M., Boellaard, E., van der Kraan, A. M., and Ponec, V., *J. Catal.* **174**, 142 (1998).
3. Grootendorst, E. J., Pestman, R., Koster, R. M., and Ponec, V., *J. Catal.* **148**, 261 (1994).
4. Tustin, G. C., Depew, L. S., and Collins, N. A., U.S. Patent 6,121,498 (2001).
5. Baro, A. M., and Erley, W., *Surf. Sci.* **112**, L759 (1981).
6. Cavalier, J. C., and Chornet, E., *Surf. Sci.* **60**, 125 (1976).
7. Rachmady, W., and Vannice, M. A., *J. Catal.* **192**, 322 (2000).
8. Pestman, R., Koster, R. M., Pieterse, J. A. Z., and Ponec, V., *J. Catal.* **168**, 255 (1997).
9. Sorensen, K., Internal Report No. 1. Laboratory of Applied Physics II, Technical University of Denmark, 1972.
10. Hummel, A. A., Badani, M. V., Hummel, K. E., and Delgass, W. N., *J. Catal.* **139**, 392 (1993).
11. Mao, C.-F., and Vannice, M. A., *J. Catal*. **154**, 230 (1995).
12. Gorte, R. J., *J. Catal.* **75**, 164 (1982).
13. Yuen, S., Chen, Y., Kubsh, J. E., Dumesic, J. A., and Topsøe, N., and Topsøe, H., *J. Phys. Chem.* **86**, 3022 (1982).
14. Jung, H.-J., Vannice, M. A., Mulay, L. N., Stanfield, R. M., and Delgass, W. N., *J. Catal.* **76**, 208 (1982).
15. Bernas, H., and Campbell, I. A., *J. Phys. Chem. Solids* **28**, 17 (1967).
16. Badani, M. V., and Delgass, W. N., *J. Catal.* **187**, 506 (1999).
17. Jackson, S. D., Kelly, G. J., and Lennon, D., *React. Kinet. Catal. Lett.* **70**, 207 (2000).
18. Itoh, K., and Bernstein, H. J., *Can. J. Chem.* **34**, 170 (1956).
19. Nakamoto, K., "Infrared and Raman Spectra of Inorganic and Coordination Compounds," 4th ed. Wiley, New York, 1986.
20. Young, R. P., and Sheppard, N., *J. Catal.* **7**, 223 (1967).
21. Rachmady, W., and Vannice, M. A., *J. Catal.*, in press.
22. Kock, A. J. H. M., and Geus, J. W., *Progr. Surf. Sci.* **20**(3), 165 (1985).
23. Vannice, M. A., Lam, Y. L., and Garten, R. L., *Adv. Chem.* **178**, 25 (1979).
24. Vink, T. J., Der Kinderen, J. M., Gijzeman, O. L. J., and Geus, J. W., *Appl. Surf. Sci.* **26**, 367 (1986).
25. Vink, T. J., Sas, S. J. M., Gijzeman, O. L. J., and Geus, J. W., *J. Vac. Sci. Technol. A* **5** (4), 1028 (1987).
26. Kock, A. J. H. M., Fortuin, H. M., and Geus, J. W., *J. Catal.* **96**, 261 (1985).
27. Wielers, A. F. H., Kock, A. J. H. M., Hop, C. E. C. A., Geus, J. W., and van der Kraan, A. M., *J. Catal.* **117**, 1 (1989).
28. Cagnoli, M. V., Marchetti, S. G., Gallegos, N. G., Alvarez, A. M., Mercader, R. C., and Yeramian, A. A., *J. Catal.* **123**, 21 (1990).
29. Guczi, L., and Lázár, K., *Catal. Lett.* **7**, 53 (1990).
30. Niemantsverdriet, J. W., van der Kraan, A. M., van Dijk, W. L., and van der Baan, H. S., *J. Phys. Chem.* **84**, 3363 (1980).
31. Cressely, J., Farkhani, D., Deluzarche, A., and Kiennemann, A., *Mater. Chem. Phys.* **11**, 413 (1984).
32. Pei, Z.-F., and Ponec, V., *Appl. Surf. Sci.* **103**, 171 (1996).
33. Doornkamp, C., and Ponec, V., *J. Mol. Catal. A* **162**, 19 (2000).